Partially Differentiated Neuroretinal Cells Promote Maturation of the Retinal Pigment Epithelium

Deepti Singh,[1,2] Xiaoyu Chen,[1–3] Tina Xia,[1,2] Maryam Ghiassi-Nejad,[1,2] Laurel Tainsh,[1,2] Ron A. Adelman,[2] and Lawrence J. Rizzolo[1,2]

[1]Department of Surgery, Yale School of Medicine, Yale University, New Haven, Connecticut, United States
[2]Department of Ophthalmology and Visual Sciences, Yale School of Medicine, Yale University, New Haven, Connecticut, United States
[3]Department of Ophthalmology, Second Xiangya Hospital, Central South University, Changsha, Hunan, China

Correspondence: Lawrence Rizzolo, Department of Surgery, Yale School of Medicine, Yale University, P.O. Box 208062, New Haven, CT 06520-8062, USA; lawrence.rizzolo@yale.edu.
DS Current address: Schepens Eye Research Institute of Massachusetts Eye and Ear, Harvard Medical School, Boston, Massachusetts, United States.

Received: June 25, 2020
Accepted: October 15, 2020
Published: November 5, 2020

Citation: Singh D, Chen X, Xia T, et al. Partially differentiated neuroretinal cells promote maturation of the retinal pigment epithelium. *Invest Ophthalmol Vis Sci.* 2020;61(13):9. https://doi.org/10.1167/iovs.61.13.9

Purpose. Many studies have demonstrated the ability of the retinal pigment epithelium (RPE) to foster the maturation of the developing retina. Few studies have examined the reciprocal effects of developing retina on the RPE.

Methods. RPE isolated from human fetal RPE or differentiated from human stem cells was cultured on Transwell filter inserts. Retinal progenitor cells (RPCs) were differentiated from human stem cells and cultured on a planar scaffold composed of gelatin, chondroitin sulfate, hyaluronic acid, and laminin-521. Cultures were analyzed by quantitative RT-PCR, immunofluorescence, immunoblotting, and transepithelial electrical resistance (TER).

Results. RPCs initially differentiated into several retina-like cell types that segregated from one another and formed loosely organized layers or zones. With time, the presumptive photoreceptor and ganglion cell layers persisted, but the intervening zone became dominated by cells that expressed glial markers with no evidence of bipolar cells or interneurons. Co-culture of this underdeveloped retinoid with the RPE resulted in a thickened layer of recoverin-positive cells but did not prevent the loss of interneuron markers in the intervening zone. Although photoreceptor inner and outer segments were not observed, immunoblots revealed that co-culture increased expression of rhodopsin and red/green opsin. Co-culture of the RPE with this underdeveloped retinal culture increased the TER of the RPE and the expression of RPE signature genes.

Conclusions. These studies indicated that an immature neurosensory retina can foster maturation of the RPE; however, the ability of RPE alone to foster maturation of the neurosensory retina is limited.

Keywords: biomaterials, human embryonic stem cells, human induced pluripotent stem cells, photoreceptors, retinal progenitor cells, retinal pigment epithelium

Retinal degeneration is a major cause of visual impairment that affects millions worldwide. Two major disorders are age-related macular degeneration and retinitis pigmentosa.[1] Retina-like organoids derived from stem cells have proven invaluable for disease modeling in culture. Stem cells can be readily differentiated into retinal precursor cells (RPCs). Great success has been achieved by creating spherical retinal organoids that mimic retinogenesis.[2–10] The retinal organoids are laminated and have been used to study mechanisms of retinal disease by producing them from patient-derived induced pluripotent stem cells.[11–15] Nonetheless, the spherical retinoid lacks the anatomical relationship of a planar neurosensory retina with its outer surface opposed to the apical surface of the retinal pigment epithelium (RPE). The re-establishment of a pseudo-subretinal space would allow for RPE–RPC contact and the concentration of factors secreted into that space.

Previous studies have demonstrated the value of reconstituting RPE–neurosensory retina interactions. It is well known that RPE cell contact or secretions, such as pigment epithelium-derived factor, affect the neurosensory retina.[16–19] Recent studies have demonstrated the importance of cell–cell contact in fostering the differentiation of human retinal organoids.[18] The retinal organoids were seeded on top of a monolayer of primary cultures of RPE that were isolated from mice. The retinal organoids of varying stages of development were added for 2 weeks. In early stages of differentiation, the RPE accelerated the expression of recoverin. When added to RPE after 5 months, retinoid cultures accelerated the expression of rhodopsin and red/green opsin. An RPE-conditioned medium had little effect, indicating that close apposition of the RPE and retinal organoids was required. A second approach with human induced pluripotent stem cell (hiPSC)-derived tissue used a microchip and fluid dynamics to recreate the choroid–RPE–neuroretina interfaces.[20] This study also cultured preformed spherical retinoids with RPE but in a chamber that mimicked choroidal blood flow. In addition to corroborating the findings of Akhtar et al.,[18] the authors demonstrated

physiological interactions between the retinoid and the RPE, such as phagocytosis of outer segments.

Conversely, a chick model of development demonstrated that the developing neurosensory retina affects differentiation and maturation of the RPE. A conditioned medium from the developing neurosensory retina promoted the differentiation of tight junctions.[21,22] Further, the conditioned medium affected the expression of a broad array of RPE mRNAs.[23] Other aspects of RPE polarity required cell–cell contact with the neurosensory retina.[24,25] To our knowledge, these effects of the neurosensory retina on the RPE have not been studied in other species.

The current study asked two fundamental questions: Could RPEs and RPCs be cultured on a large scale if retinal organoids could be cultured as a flat sheet? Would those co-cultures further the maturation of the RPE? Attempts to culture a planar retina have used artificial materials or natural substrates found in the retina.[26–28] To date, these approaches have not been reported to yield laminar retinal organoids. Some scaffolds promoted the differentiation of RPCs into photoreceptor precursors.[27,28]

To explore these questions, we examined the following markers of retinal differentiation. LHX2, PAX6, and VSX2 are early eye field proteins found in all RPCs and subsequently in different lamina, as differentiation proceeds. PAX6 becomes a marker for retinal ganglion cells (RGCs) and VSX2 for bipolar cells.[29–31] LHX2 initially co-localizes with VSX2 and later is found in some amacrine cells and in Müller glia along with glutamine synthetase.[32] HuC/D and BRN3 are markers for RGCs. HuC/D is a cytoplasmic, RNA-binding protein,[33] and BRN3 is a transcription factor.[31] Recoverin is a neuronal calcium binding protein that is found in the cell bodies and processes of photoreceptor precursors and, when they form, the outer segments of photoreceptors.[34] CRX is a gene product of a cone–rod homeobox gene expressed by photoreceptors.[35] OTX2 is a transcription factor and is involved in the differentiation of photoreceptors and bipolar cells.[29]

We have described a scaffold composed of chondroitin sulfate, collagen, and hyaluronic acid as a mimetic of the retinal extracellular matrix.[27] The scaffold provided a niche that favored retinal differentiation over other cells of the anterior forebrain. Cells of the same cell type clustered, but lamina failed to form, and a continuous planar retinoid was not achieved.[36]

In this report, we improved the scaffold by decorating it with laminin-521, which promotes cell proliferation in stem cell niches.[37–43] Laminin-5xx (laminins with α5 subunits) is found in the inner limiting membrane throughout fetal development.[42] The scaffold-cultured RPCs were co-cultured with RPE, and we examined the effects of co-culture on the differentiation of each "tissue."

Materials and Methods

See Supplementary Materials for complete methods.

Cells

Human embryonic stem cells (hESCs), WA09, were obtained from WiCell Research Institute (Madison, WI, USA). We obtained the hiPSCs Y6 and IMR90-4 from Yale University Stem Cell Center (New Haven, CT, USA) and WiCell, respectively. Human fetal RPE (hfRPE) was a gift of A. Mamaniskis and S. Miller (National Eye Institute, National Institutes of Health, Bethesda, MD, USA).

Differentiation and Culture of RPCs on the GCH-521 Scaffold

Undifferentiated stem cells were maintained and differentiated as described previously.[9] On day 21 (D21), retinal vesicles were harvested and maintained in suspension culture or dissociated and plated on the GCH-521 scaffold. The original method for fabricating the GCH scaffold[36] was modified by the addition of laminin-521. Dried GCH scaffolds were rehydrated by adding 20 µL of serum-free medium (SFM; 70% high-glucose Dulbecco's modified Eagle's medium and 30% F-12 supplemented with 2% B27 and penicillin/streptomycin) supplemented with 1.0 µg/mL laminin-521 (STEMCELL Technologies, Vancouver, BC, Canada). Scaffolds were incubated at 37°C for 30 minutes before seeding with RPCs. Cultures were maintained in SFM, and medium was changed three times per week for the rest of the experiment.

RPE and Co-Culture

RPE was derived from IMR90-4 cells and cultured as described earlier.[44,45] hfRPE was cultured as described earlier.[44] In each case, cells were seeded on Transwell culture inserts (Corning Inc., Corning, NY, USA) that were coated with 10 µg Synthemax (Corning). Six weeks post-confluence, cells were adapted to SFM. The transepithelial electrical resistance (TER) was monitored using an EVOM2 resistance meter with EndOhm electrodes (World Precision Instruments, Sarasota, FL, USA). One week after plating on GCH-521, RPC cultures were layered cell-side down onto differentiated RPE (Supplementary Fig. S1). Co-cultures were maintained up to 9 months.

Quantitative Real-Time Reverse-Transcription PCR

RNA was extracted using TRIzol reagent (Thermo Fisher Scientific, Waltham, MA, USA) and cDNA prepared as described earlier.[36] Primers for quantitative real-time reverse-transcription PCR (qRT2-PCR) are listed in Supplementary Table S1. Alternatively, cDNA was analyzed using custom-made RT-PCR microarrays (Bio-Rad, Hercules, CA, USA) (Supplementary Fig. S2). Relative mRNA expression was normalized to the housekeeping genes *ACTB* and *GAPDH*, and the $2^{-\Delta\Delta Ct}$ method was used for analysis.[46]

Immunocytochemistry and Immunoblotting

Frozen sections (12 µm) were mounted on polylysine-coated slides. Primary antibodies and secondary antibodies are listed in Supplementary Table S2. Fluorescence images were captured with an LSM 410 spinning-disc confocal microscope and processed using Zen software (Carl Zeiss SBE, LLC, Thornwood, NY, USA). The images are representative of three or more experiments. The windows for color channels were determined by the sample with the greatest signal intensity and applied uniformly to all related images in that figure.

Protein extracts were resolved by sodium dodecyl sulfate–polyacrylamide gel electrophoresis and followed by immunoblotting. Actin was used as an internal standard to

Investigative Ophthalmology & Visual Science

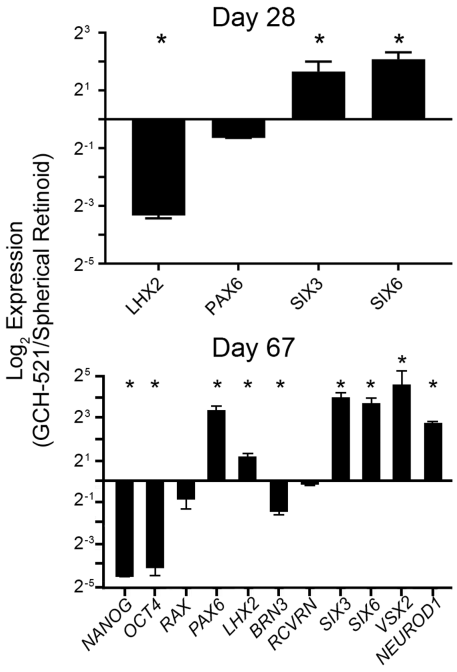

Figure 1. Laminin-521 promoted the differentiation of WA09-derived RPCs. RPCs were isolated on D21 and maintained as retinal spheroids or plated on GCH-521. Gene expression was assayed by qRT^2-PCR. (**A**) One week after plating, expression of mRNA was elevated for GCH-521 cultures relative to retinal spheroids for the early eye-field gene *SIX3* but depressed for *LHX*. *SIX6*, which typically appears between D25 and D28, was also elevated in the GCH-521 cultures. (**B**) By D67, expression of the pluripotency markers *OCT4* and *NANOG* was substantially lower. Expression was elevated for *PAX6*, *SIX3*, *SIX6*, *VSX2*, and *NEUROD1*. $^*P < 0.05$ for three independent experiments.

normalize each sample. Details of the antibodies used are in Supplementary Table S2. Blots were imaged using a Chemi-Doc MP Imaging System (Bio-Rad).

Statistical Analysis

All statistical data are presented as the mean ± standard error, unless otherwise stated. Independent cultures from both cell lines were analyzed in triplicate. Comparisons were made using one-way ANOVA, and $P < 0.05$ was considered statistically significant.

Results

Monoculture of RPCs

The cultures on scaffolds were compared to spherical retinal spheroids of comparable age. Embryoid bodies were differentiated for 21 days (D21) to form retinal vesicles and express early eye-field transcription factors. Retinal vesicles were isolated, and the cells were dissociated and seeded onto GCH-521 scaffolds. Compared with the spherical retinal organoids, cultures on GHC-521 enhanced the expression of some genes but not others. One week after plating, expression of the mRNAs increased for the early eye-field genes *SIX3* and *SIX6* but decreased for *LHX2* ($P < 0.05$) (Fig. 1). On D67 (46 days post-seeding), the mRNAs increased for *VSX2*, *NEUROD1*, *PAX6*, *SIX3*, and *SIX6* ($P < 0.05$). Expression decreased for the mRNAs of the stem cell markers *NANOG* and *OCT4* ($P < 0.05$).

Protein expression was followed by indirect immunofluorescence of frozen sections. On D42 (21 days post-seeding), an ~150-µm-thick layer of cells was observed on one side of the ~85-µm-thick autofluorescent scaffold (Fig. 2). We examined the products of the early eye-field genes *PAX6*, *VSX2*, and *LHX2*. A low-power view revealed PAX6 in a zone of cells on the free surface and in cells near the scaffold. As in the example of Figure 2, an island of PAX6 cells was occasionally found between these surfaces. VSX2 and LHX2 were most evident in an intermediate zone between the two layers of PAX6. They were absent from the island of PAX6 noted above. A few LHX2- and VSX2-positive cells were found on the scaffold and free surfaces but were distinct from the PAX6-positive cells. It appeared that different cell types were segregating from one another into loosely formed lamina.

By D51, evidence of photoreceptor precursors was suggested by positive signals for OTX2, CRX, and recoverin (RCVRN) near the free surface (Fig. 3). Recoverin immunoreactivity localized to the cytoplasm of cells that expressed OTX2 immunoreactivity in the nucleus. Recoverin immunoreactivity was absent from some OTX2-postive cells. CRX was found predominantly in the nucleus but also in the cytoplasm of some cells.

By D70, the ganglion cell-associated markers HuC/D and BRN3 were found in cells that were enriched near the scaffold (Fig. 3). HuC/D was found in the cytoplasm and BRN3 in the nucleus. Recoverin was detected in the perinuclear cytoplasm of a band of cells adjacent to the free surface. Short processes were observed, but inner or outer segments were not in evidence. A zone of nuclei that was unlabeled by any of these markers lay between them.

Between 3 and 6 months, differentiation of the cultures failed to form elongated precursors of photoreceptors or bipolar cells, as would spherical retinoids. Longer cultures (up to 9 months) were no different than 6-month cultures. The cultures were as thick as 1000 µm, and an ~100- to 200-µm-thick zone of recoverin immunopositive cells was found at the free surface of the culture (Fig. 4A). The boundary between the recoverin and underlying zone was ragged. Flat mounts demonstrated that the recoverin-positive cells extended long processes (Fig. 4B). HuC/D-positive cells were observed near the scaffold, but they were few in number relative to the number of nuclei. The thick, intervening zone was dominated by cells with immunoreactivity for glutamine synthetase. There was little if any immunoreactivity for markers of bipolar cells or interneurons. Live cultures labeled with Tubulin Tracker (Thermo Fisher Scientific) demonstrated several layers of neurite-like processes that ran parallel to the plane of the monolayer (Fig. 4C). Opsin- or rhodopsin-positive cells were scarce and lacked the morphology of photoreceptors.

Co-Culture of RPCs with RPE

On day 21, RPCs were plated on GCH-521. Three days later they were co-cultured with hfRPE or hiPSC-derived RPE. By the time the scaffold with RPCs was added to the RPE culture, RPE had been >8 weeks post-confluent and adapted to SFM. The cultures were followed for up to 9 months. At 3 months, the metabolic activity of the co-culture, as measured by the alamarBlue Assay (Thermo Fisher Scientific), equaled the combined activity of RPE alone plus RPCs alone (Supplementary Fig. S3); therefore, cells from both

Investigative Ophthalmology & Visual Science

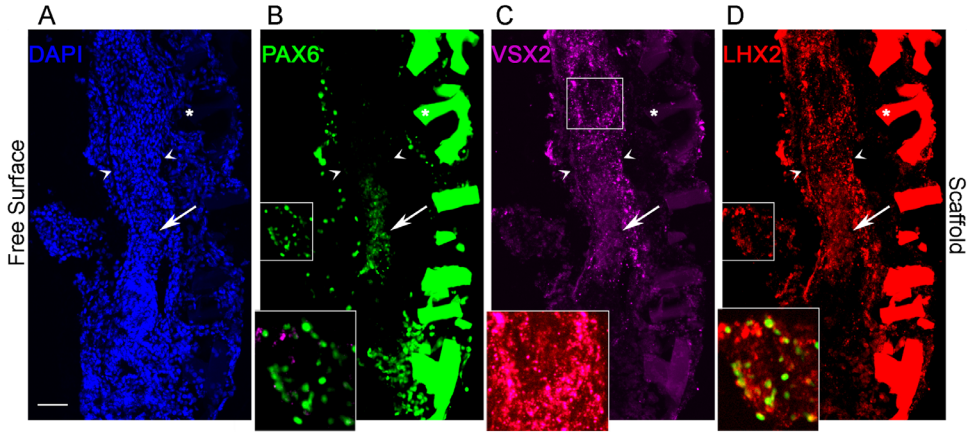

Figure 2. By D42, RPCs on the GCH-521 scaffold formed discontinuous zones. A low-power micrograph shows an ~175 µm-thick layer of cells sitting on the GCH 521 scaffold. The same sample was immunolabeled with antibodies to PAX6 (*green*), LHX2 (*magenta*), and VSV2 (*red*). Boxes indicate regions that were magnified 4× for the insets, which exhibit two of the color channels. (**A**) Cell nuclei were stained with 4′,6-diamidino-2-phenylindole (DAPI) (*blue*) to reveal all the cells in the tissue. (**B**) PAX6 immunoreactivity was found in zones near the free surface and in and about the autofluorescent scaffold (*asterisks*). An island of immunoreactivity was found between these layers (*arrow*). (**C**, **D**) VSX2 and LHX2 immunoreactivity was primarily found in an intermediate zone. VSX2- and LHX2-positive cells that were found in the free surface zone were distinct from PAX6-positive cells and, using PAX6 as a reference, were distinct from each other (insets, **B** and **D**). The intermediate zone exhibited VSX2 and LHX2 immunoreactivity (inset, **C**). Images are representative of three independent experiments, each with WA09- and Y6-derived cultures. *Arrows* indicate the same position in each panel. Paired *arrowheads* delineate the intermediate zone and indicate the same position in each panel. *Scale bar*: 50 µm.

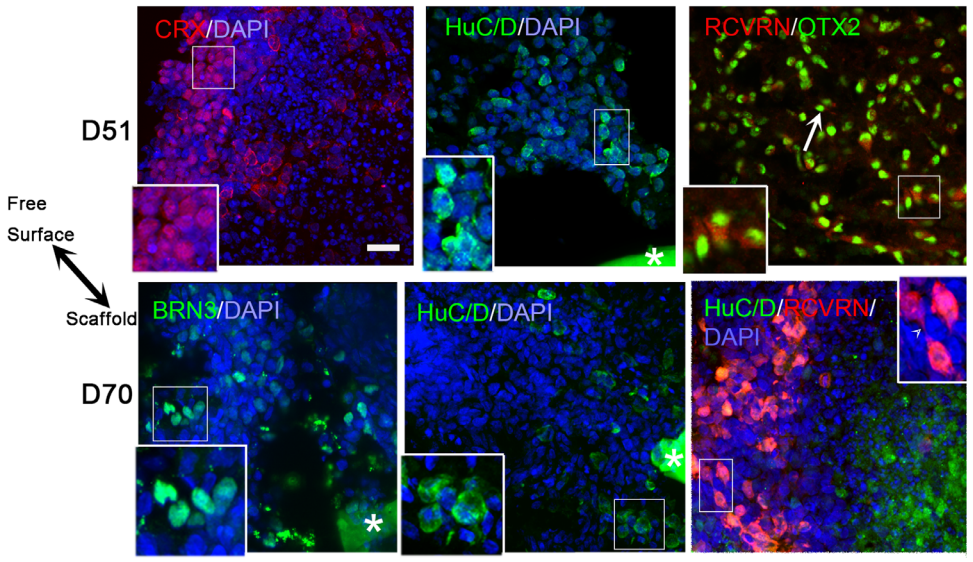

Figure 3. At later stages of differentiation, like cells formed clusters that lay either in the free or scaffold zones. Frozen sections from various samples were prepared on days 51 and 70. The scaffold (*asterisks*) is out of the frame of panels that focus on PR precursors; the *double-headed arrow* indicates the orientation of all the panels except D51: RCVRN/OTX2. That panel shows a grazing section through the free surface. On D51, CRX immunoreactivity was observed in the nucleus of cells near the free surface. The cells overlay a layer of unlabeled cells that separated CRX-positive cells from the RGC-like layer, which is out of the field of view. HuC/D immunoreactivity was observed in the perinuclear cytoplasm of cells near the scaffold; the free surface is out of the field of view. RCVRN and OTX2 labeled the same cells near the free surface. OTX2 immunoreactivity was found in the nucleus and RCVRN in the cytoplasm (inset). In some cells, only OTX2 immunoreactivity was evident (*arrow*). On D70, HuC/D and BRN3 were evident near the scaffold. HuC/D immunoreactivity was found in the perinuclear cytoplasm, whereas BRN3 was found in the nucleus. In the right-hand panel, HuC/D-labeled cells were separated from RCVRN by a zone of non-immunoreactive cells. Images are representative of two independent experiments each with WA09- and Y6-derived cultures. Insets are a 4× enlargement of the associated panel. *Scale bar*: 20 µm.

cultures appeared to be metabolically active. The cultures of RPCs on the GCH-521 scaffold failed to exhibit an appreciable TER (Fig. 5A). The TER of the monocultures was consistent with other reports for hiPSC-RPE.[47–49] Due to co-culture, the TER of both hfRPE and hiPSC-derived RPE increased significantly ($P < 0.01$). Co-culture did not affect the morphology of the RPE as assessed by indirect immunofluorescence (Fig. 5B). Polygonal monolayers were observed in the *x*,*y* plane, with circumferential bands of ZO-1 and actin. In the *x*,*z* plane, ZO-1 and actin were observed in

Investigative Ophthalmology & Visual Science

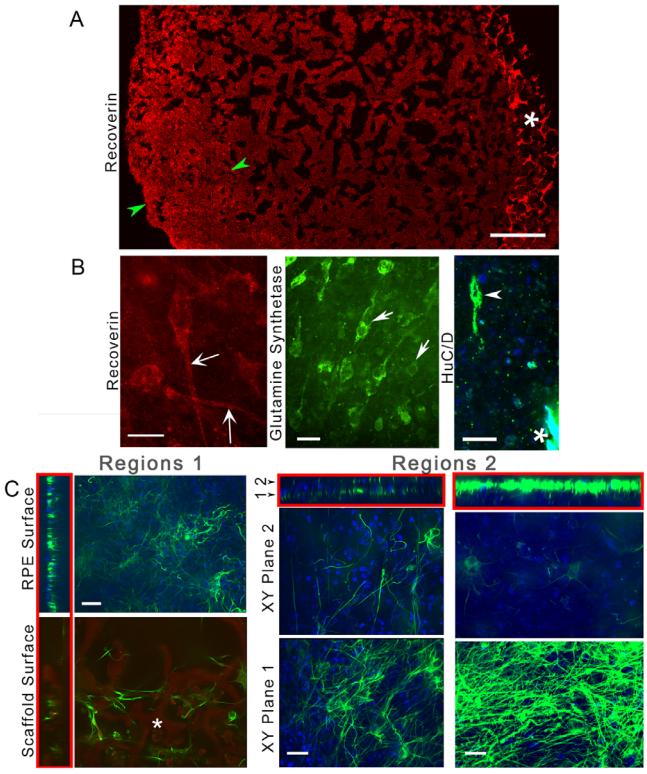

Figure 4. Six- to 8-month cultures of IMR90-4-derived RPCs expressed immunoreactivity for recoverin in the free surface zone, HuC/D in the scaffold zone, and glutamine synthetase throughout the tissue. (**A**) Frozen sections of 7-month cultures were fluorescently labeled with antibodies to recoverin. The autofluorescent scaffold (*asterisk*) is seen along the left border of the image and the free surface along the right border. A thick layer of recoverin-positive cells (*green arrowheads*) was evident along the free surface. Background staining of the intervening region revealed the continuity of the cells; dark spaces between the cells are sectioning artifacts. (**B**) Flat mounts were prepared from 8-month cultures. Confocal slices are aligned with the free surface, intermediate, and peri-scaffold regions of panel **A**. Slices near the free surface revealed recoverin in the cell body and long, thin processes (*long arrows*). Slices near the scaffold (*asterisk*) revealed that HuC/D immunoreactivity was observed in the cell body and long thin processes of some cells (*arrowheads*). Slices between these zones revealed glutamine synthetase in cell bodies (*short arrows*) and extended processes. (**C**) Tubulin tracker was added to both sides of live, 6-month cultures and imaged by confocal microscopy. The dye was unable to penetrate the thickness of the culture. The *x,z* sections are boxed in *red*. Regions 1: Cultures were mounted with the either the free surface or the scaffold surface adjacent to the coverslip; confocal slices were taken through the free and scaffold zones, and neurite-like processes were evident in each zone. Regions 2: Two optical sections within the free surface zone revealed two layers of neurite-like processes; sections were counterstained with DAPI (*blue*). Images are representative of three experiments. Similar results were observed with 9-month cultures. *Scale bars*: A, 200 µm; B and C, 20 µm.

an apical junctional complex at the apical end of the lateral membranes.

To further assess the effects of co-culture, we used two RT-PCR microarrays, one for the RPE layer and a second for the RPC layer. The first array assayed a subset of signature genes and markers of RPE maturation (Fig. 6A).[44,50] Gene expression of a subset of signature genes for RPE increased because of co-culture (*BEST1*, *DCT*, *FRZB*, *MET*, *MITF*, *MYRIP*, *PMEL*, *RBP1*, and *SFRP5*), along with two genes *SLC22AB* and *PCDHGD4*, which are makers for RPE maturation. The second array assayed a representative collection of retinal markers and a few RPE markers to access cross-contamination. The results were mixed. Gene expression increased for early eye-field/photoreceptor genes (*RAX* and *SIX3*) and retinal markers, including photoreceptors (*NR2E*, *GNAT*, *PRPH2*, *RCVRN*, and *THRB*), retinal ganglion cells (*POUAF1* and *POUAF2*), and interneurons (*PROX1*) (Fig. 6B). Gene expression decreased for some markers, including photoreceptors (*OPN1SW*), retinal ganglion cells (*ELAVL4*, *NEFM*, and *PVALB*), and interneurons/bipolar cells (*CALB2*, *DLG4*, *GAD1*, and *PCKα*).

Frozen sections of D90 cultures were prepared by first separating the RPE and neuronal layers, as the Transwell filter is difficult to section. Co-culture with the RPE resulted in a thick layer of recoverin-positive cells, up to 10 to 15 cells deep, that exhibited a sharp boundary with the intermediate zone (Fig. 7). There was no evidence of an outer plexiform layer or cellular extensions into the intermediate zone. The intermediate zone is where we would expect to find bipolar cells, or other interneurons, and Müller cells. An early eye-field marker that is also associated with Müller cells, LHX2, was detected in this zone; LHX2 was sparse in and about the scaffold where retinal ganglion cell markers were found. Like the monocultures, there was no evidence of interneurons.

Immunoblotting revealed the presence of rhodopsin and R/G opsin in the 6-month co-cultures (Fig. 8). Rhodopsin was undetected in the monocultures and showed a strong signal on the immunoblots from co-culture preparations. A doublet was observed for red/green (R/G) opsin in mono- and co-cultures. The doublet might result from variable posttranslational modification.[51,52] Co-cultures appeared to increase the amount of R/G opsin. Unlike the opsins, co-culture had no apparent effect on the expression of HuC/D or glutamine synthetase. Neither VSX2 nor PROX1 was detected in mono- or co-cultures. In frozen sections, we did not observe convincing evidence of rhodopsin- or opsin-positive cells or any morphological evidence of inner and outer segments.

Discussion

The best culture models of the neurosensory retina are based on protocols that differentiate iPSCs into spherical retinoids, and we compare our findings with this literature.[53–55] The retinoids often include a tuft of RPE, but RPE is not essential. When present, the RPE is in an ectopic location, although it could contribute secretory products that are known to enhance differentiation.[16–19] The timing of developmental events varies among cell lines and protocols, but the order of events is roughly the same. Rather than time in culture, Caposki et al.[56] related developmental landmarks to three morphological stages. The order of events and the range for their appearance in culture is summarized in Figure 9 and compared to our findings. Briefly, after early eye-field genes are expressed, a layer of retinal ganglion cells appears along the luminal surface of the spheroid along with neurofilaments. Subsequently, distinct layers appear with markers for photoreceptor precursors on the outer surface and interneurons in the region between the photoreceptor and ganglion cell markers. Cells positive for photoreceptor markers elongate. Patches of photoreceptors with inner and outer segments increase in size as evidence of the RGC layer

Investigative Ophthalmology & Visual Science

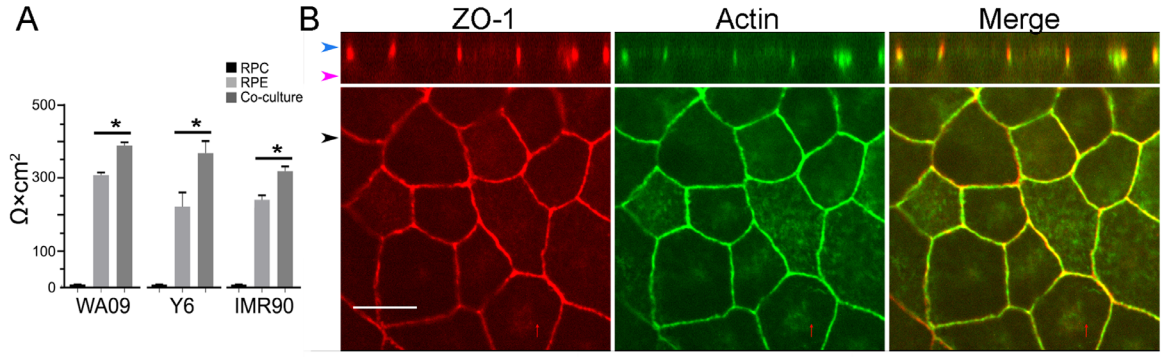

Figure 5. Co-culture increased the TER of RPE. WA09- and Y6-derived RPC cultures were co-cultured with hfRPE. IMR90-4 RPC-derived cultures were co-cultured with IMR90-4-derived RPE. (**A**) The TER of RPC-derived monocultures (*black*) was negligible. For each 3-month co-culture (*dark gray*), the TER was significantly higher than parallel monocultures (*light gray*) ($P < 0.01$). (**B**) Following the TER measurement, the morphology of the RPE was examined by indirect immunofluorescence after the scaffold and RPC-derived tissue were removed. The large panel at the bottom of the image is the *x,y* plane, and the thin panel at the top is the *x,z* plane. The *black arrowhead* indicates the plane of section for the *x,z* plane. The *blue arrowhead* indicates the position of the apical membrane, and the *magenta arrowhead* indicates the base of the monolayer. A typical polygonal lattice was observed in the *x,y* plane. In the *x,z* plane, ZO-1 (tight junctions) overlapped with actin (both tight and adherens junctions) to form an apical junctional complex, which localized to the apical end of the lateral membranes. $^{*}P < 0.01$ ($n = 3$). *Scale bar*: 20 µm.

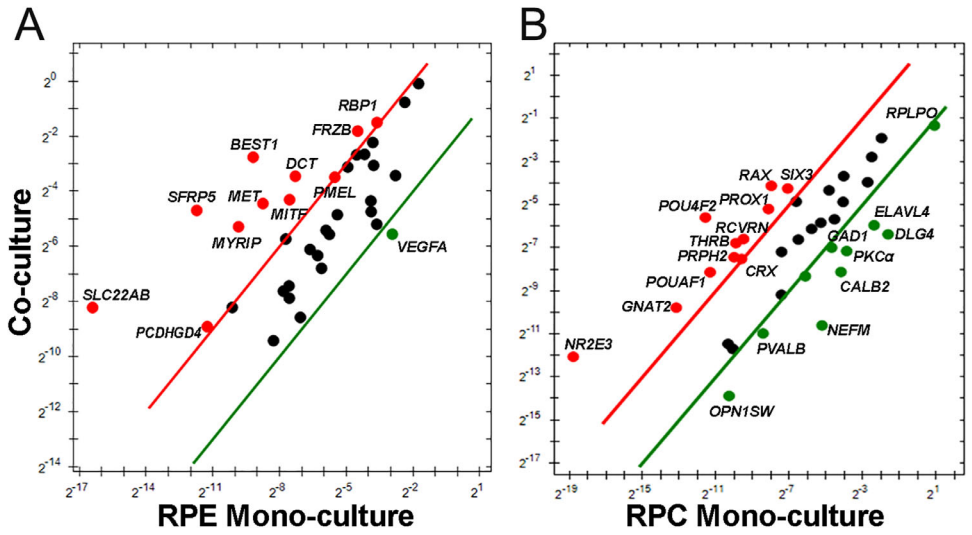

Figure 6. Co-culture of WA09-derived RPE and RPCs affects the differentiation of each culture. Co-culture affected the expression of mRNAs for a subset of RPE (**A**) and retinal (**B**) markers. Expression of transcripts above the *red line* increased by more than four times and those below the *green line* decreased by more than four times ($n = 3$).

decreases. Morphologic and immunocytochemical evidence of synapses appear, and light-evoked electrical signals can be detected. The entire process requires 6 to 9 months.

Differentiation of RPC Monocultures

Planar culture models of the neurosensory retina would offer several advantages. Investigators could readily access both sides of the culture. Ganglion cells might survive longer due to better access to nutrients and more space for axons to grow; however, this was not observed. Conceivably, RGCs died due to lack of electrical stimulation or the absence of a target cell. We could not detect neurites oriented perpendicular to the scaffold and found no evidence of synapses. Further, there were no astrocytes or endothelial cells whose secretions might have stabilized the inner layers. Another confounding factor is that the cultures were likely contaminated with RPE and derivatives of anterior forebrain precursors. Unlike retinal spheroids, we were unable to select spheroids with an RPC morphology. The occasional island of PAX6-positive cells between the surface and scaffold layers might reflect patches of these contaminants.

Compared with our earlier scaffold, the addition of laminin-521 initially improved cell attachment and fostered cell proliferation. Later it appeared to promote segregation of neuronal cell types into zones. In the first few months, cells with photoreceptor markers tended to be on the free surface and cells expressing ganglion cell markers were enriched near the scaffold. Because laminin-521 is enriched in the inner limiting membrane,[42] it might have promoted this localization of ganglion cells. If so, laminin-521 is not required, because in retinal spheroids the

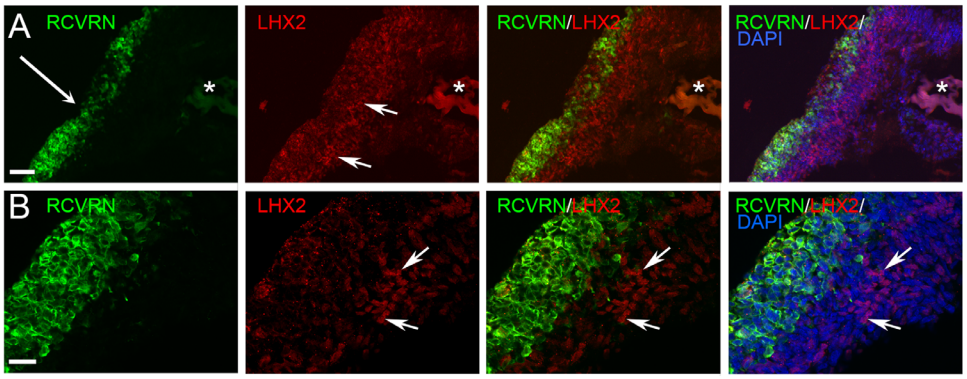

Figure 7. Co-culture sharpened the boundary of the RPE-facing zone. Co-cultures of Y6-derived RPCs with hfRPE were maintained for 3 months. The RPE was removed, and frozen sections of the RPC layer were labeled with antibodies, as indicated in each panel. The *long arrow* is perpendicular to the plane of the tissue and indicates the RPE-facing surface. The scaffold is indicated by the asterisk. (**A**) Neither antibodies to RCVRN nor LHX2 labeled cells near the scaffold. Recoverin labeled a layer of cells at the RPE-facing surface that was as much as 10 to 15 cells deep. LHX2-labeled cells (*short arrows*) were enriched in a zone adjacent to the recoverin-positive cells. (**B**) A second sample, oriented the same way, was imaged at higher magnification. There is a sharp boundary between the LHX2 and recoverin zones. *Short arrows* indicate the same LHX2-positive cells in each panel. *Scale bars*: A, 50 µm; B, 20 µm.

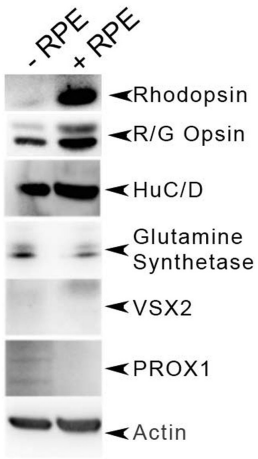

Figure 8. Co-culture increased the expression of opsins. IMR90-4-derived RPE was co-cultured with IMR90-4-derived RPCs for 6 months. Immunoblotting demonstrated the presence of a doublet for R/G opsin in monocultures that increased relative to actin as a result of co-culture. Rhodopsin was not detected in the monocultures but was evident in co-cultures. Co-culture did not affect the expression of HuC/D or glutamine synthetase. VSX2 and PROX1 were not detected under either culture condition. Blots are representative of three independent experiments.

distribution of ganglion cells is polarized long before laminin-5xx is detected.[43] Cells expressing markers for glia and interneurons were enriched in an intermediate zone. Despite similarities to differentiation in retinal spheroids, this trend was not evident throughout the culture, and the definitive lamination found in spherical retinal organoids was only partially achieved.

The presumptive RGCs diminished in density between 3 and 6 months, but they remained close to the scaffold. Markers for interneurons were absent, and glial markers dominated the intervening region, which became quite thick, ~800 µm. Despite the presence of recoverin, there was little morphological evidence of photoreceptors. Further, tubulin positive processes traveled parallel to the scaffold rather than penetrating into the tissue. Nonetheless, R/G opsin, but not rhodopsin, could be detected on immunoblots.

Differentiation of Co-Cultures

RPCs were cultured for up to 9 months with an established (i.e., high TER), planar monolayer of RPE. The hypothesis was that differentiation of RPCs would improve by restoring their normal anatomical relationship with RPE. Further, the RPCs would also advance the maturation of RPE. The pseudo-subretinal space created by co-culture would presumably concentrate secreted factors from the RPE and RPCs and enable RPE–outer retina interactions. Co-cultures were initiated early during differentiation to allow the tissues to co-differentiate, as hypothesized in Supplementary Figure S1A. A timeline for the events we observed is provided in Figure 9.

Co-culture had little effect on the differentiation of the RPCs, aside from a modest effect on photoreceptor precursors. At 3 months, there was a modest increase in the expression of genes for some retinal cell markers, but others decreased. Nonetheless, immunofluorescence revealed a thickened zone of recoverin-positive cells on the RPE-facing surface that overlay a zone of LHX2-positive cells. This localization at this stage of differentiation would be consistent with the role of LHX2 in regulating the differentiation of interneurons.[57]

By 6 months, immunoreactivity remained for recoverin in cell bodies along the RPE surface of the retinal culture. Co-culture had little effect on RGCs and intermediate cell layers. Although immunoblots revealed an increase in expression of R/G opsin and rhodopsin became evident, immunofluorescence failed to reveal cells with a convincing morphology of photoreceptors. These data do not replicate, but are consistent with, studies of human spherical retinal organoids seeded on a monolayer of mouse RPE or on a monolayer of hiPSC–RPE in a microchip chamber.[18,20] Those studies seeded the RPE cultures with retinal spheroids that had already formed interconnected retinal lamina. In that circumstance, contact with the RPE accelerated the differentiation of photoreceptors. They did not address effects on

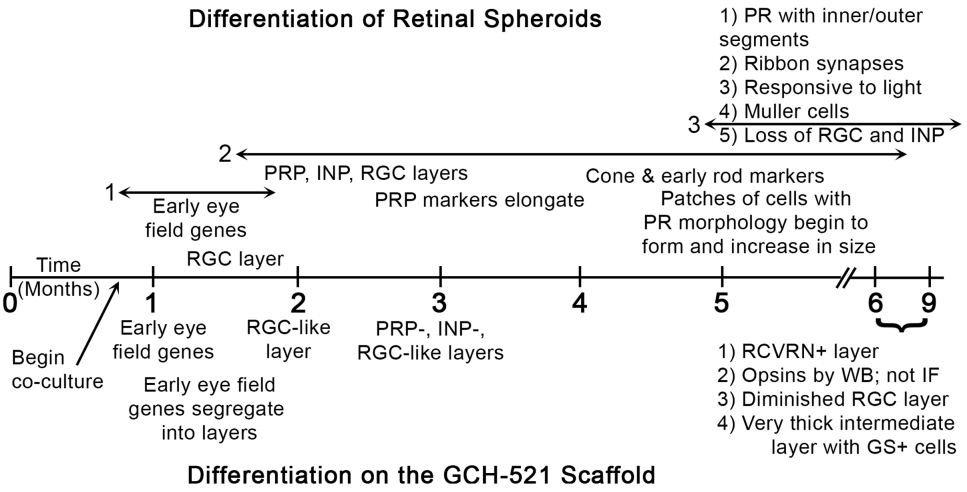

Figure 9. Differentiation of RPC in culture. The timeline is in months. Above the timeline, the differentiation of retinal spheroids combines data from several studies.[53–56] All times are rough approximations, as they vary with cell line and culture protocol. The double-headed arrows indicate the ranges of the three stages described by Capowski et al.[56] The characteristics of stages 1 and 2 are shown below the *arrows*. The characteristics of stage 3 lie on either side of the *arrow*. Below the timeline are approximate times for events observed in the current study.

other retinal neurons. Our study demonstrated that anatomically placed RPE did not replace the cocktail of supplements that others have used to promote differentiation of RPCs.[18,20,56,58,59] If placed in the basal medium chamber of the culture, RPE might transport these supplements to the retinal cells as part of its native barrier functions.[58] This approach might achieve our initial goal of creating a large-scale RPE/neurosensory retinoid with properties comparable to the micro-retinoid developed by Achberger et al.[20]

For RPE, RPCs derived from three stem cell lines matured the barrier function of RPE, as evidenced by an increase in the TER of hiPSC-derived RPE and hfRPE isolated from 15- to 16-week-gestation fetuses. There was also an increase in the expression of genes that define RPE.[50,60] These included genes for melanin formation, Wnt signaling, and membrane transport.

The first evidence that the developing neurosensory retina influenced the maturation of RPE was from studies of chick embryogenesis.[21–23,61] Diffusible factors from the developing neurosensory retina affected the expression of numerous genes and increased the TER by fostering the development of tight junctional strands. The active agents secreted by conditioned medium prepared from embryonic day 7 (E7) retinas (no retinal lamina present) differed from those secreted by E14 retinas (photoreceptors with only inner segments). Concomitant with this stepwise increase in TER, cell–cell contact polarized the distribution of several proteins.[24,25] In humans, RPEs isolated from 13-week-gestation fetuses have high TER.[62] By this time, ganglion cell and inner plexiform layers have developed, but the outer plexiform layer continues to develop through week 18.[63] Rudimentary inner segments of the photoreceptors are evident at 26 weeks.[64] Together with the current study, the immature neurosensory retina apparently modulates maturation of the outer blood–retinal barrier in species as divergent as chickens and humans.

These data support the hypothesis that, early in development, the presumptive neurosensory retina begins to promote maturation of the RPE. The maturing RPE feeds back to enhance differentiation of the outer retina. Absent a choroid or choroidal blood supply and astrocytes and endothelial cells, feedback in our model was limited to modest effects on the putative photoreceptor layer. The choroid contains factors that foster the differentiation of the neurosensory retina (e.g., serum, retinoic acid, taurine). By adding such factors to the basal medium chamber, planar co-cultures would provide a model to probe mechanisms whereby the outer blood–retinal barrier influences differentiation of the neurosensory retina.

Acknowledgments

The authors thank W.J. Brunken, PhD (Upstate Medical University, New York) for the suggestion of laminin-521.

Supported by the Connecticut Regenerative Medicine Research Fund (14-SCB-YALE-18, LJR), Department of Defense (W81XWH-15-1-0029, LJR), Yale School of Medicine Richard K. Gershon Student Research Fellowship (MG-N), National Institutes of Health (TL1 TR000141, LT), National Institutes of Health and Yale School of Medicine Medical Student Research Fellowships (TX), Alonzo Family Fund (LJR), Newman's Own Foundation and Leir Foundation (RAA), and Research to Prevent Blindness (Yale University).

Disclosure: **D. Singh,** None; **X. Chen,** None; **T. Xia,** None; **M. Ghiassi-Nejad,** None; **L. Tainsh,** None; **R.A. Adelman,** None; **L.J. Rizzolo**, None

References

1. Wert KJ, Lin JH, Tsang SH. General pathophysiology in retinal degeneration. *Dev Ophthalmol*. 2014;53:33–43.
2. Mellough CB, Collin J, Khazim M, et al. IGF-1 signaling plays an important role in the formation of three-dimensional laminated neural retina and other ocular structures from human embryonic stem cells. *Stem Cells*. 2015;33(8):2416–2430.
3. Meyer JS, Howden SE, Wallace KA, et al. Optic vesicle-like structures derived from human pluripotent stem cells facilitate a customized approach to retinal disease treatment. *Stem Cells*. 2011;29(8):1206–1218.

4. Meyer JS, Shearer RL, Capowski EE, et al. Modeling early retinal development with human embryonic and induced pluripotent stem cells. *Proc Natl Acad Sci USA*. 2009;106(39):16698–16703.
5. Nakano T, Ando S, Takata N, et al. Self-formation of optic cups and storable stratified neural retina from human ESCs. *Cell Stem Cell*. 2012;10(6):771–785.
6. Ohlemacher SK, Iglesias CL, Sridhar A, Gamm DM, Meyer JS. Generation of highly enriched populations of optic vesicle-like retinal cells from human pluripotent stem cells. *Curr Protoc Stem Cell Biol*. 2015;32:1H.8.1–1H.8.20.
7. Reichman S, Terray A, Slembrouck A, et al. From confluent human iPS cells to self-forming neural retina and retinal pigmented epithelium. *Proc Natl Acad Sci USA*. 2014;111(23):8518–8523.
8. Eiraku M, Takata N, Ishibashi H, et al. Self-organizing optic-cup morphogenesis in three-dimensional culture. *Nature*. 2011;472(7341):51–56.
9. Zhong X, Gutierrez C, Xue T, et al. Generation of three-dimensional retinal tissue with functional photoreceptors from human iPSCs. *Nat Commun*. 2014;5:4047.
10. Kaewkhaw R, Swaroop M, Homma K, et al. Treatment paradigms for retinal and macular diseases using 3-D retina cultures derived from human reporter pluripotent stem cell lines. *Invest Ophthalmol Vis Sci*. 2016;57(5):ORSFl1–ORSFl11.
11. Tucker BA, Mullins RF, Streb LM, et al. Patient-specific iPSC-derived photoreceptor precursor cells as a means to investigate retinitis pigmentosa. *Elife*. 2013;2:e00824.
12. Arno G, Agrawal SA, Eblimit A, et al. Mutations in REEP6 cause autosomal-recessive retinitis pigmentosa. *Am J Hum Genet*. 2016;99(6):1305–1315.
13. Burnight ER, Wiley LA, Drack AV, et al. CEP290 gene transfer rescues Leber congenital amaurosis cellular phenotype. *Gene Ther*. 2014;21(7):662–672.
14. Parfitt DA, Lane A, Ramsden CM, et al. Identification and correction of mechanisms underlying inherited blindness in human iPSC-derived optic cups. *Cell Stem Cell*. 2016;18(6):769–781.
15. Ohlemacher SK, Sridhar A, Xiao Y, et al. Stepwise differentiation of retinal ganglion cells from human pluripotent stem cells enables analysis of glaucomatous neurodegeneration. *Stem Cells*. 2016;34(6):1553–1562.
16. Kolomeyer AM, Sugino IK, Zarbin MA. Characterization of conditioned media collected from aged versus young human eye cups. *Invest Ophthalmol Vis Sci*. 2011;52(8):5963–5972.
17. Zhu D, Deng X, Spee C, et al. Polarized secretion of PEDF from human embryonic stem cell-derived RPE promotes retinal progenitor cell survival. *Invest Ophthalmol Vis Sci*. 2011;52(3):1573–1585.
18. Akhtar T, Xie H, Khan MI, et al. Accelerated photoreceptor differentiation of hiPSC-derived retinal organoids by contact co-culture with retinal pigment epithelium. *Stem Cell Res*. 2019;39:101491.
19. Yanai A, Laver CRJ, Gregory-Evans CY, Liu RR, Gregory-Evans K. Enhanced functional integration of human photoreceptor precursors into human and rodent retina in an ex vivo retinal explant model system. *Tissue Eng Part A*. 2015;21(11–12):1763–1771.
20. Achberger K, Probst C, Haderspeck J, et al. Merging organoid and organ-on-a-chip technology to generate complex multi-layer tissue models in a human retina-on-a-chip platform. *Elife*. 2019;8:e46188.
21. Ban Y, Rizzolo LJ. A culture model of development reveals multiple properties of RPE tight junctions. *Mol Vis*. 1997;3:18.
22. Ban Y, Wilt SD, Rizzolo LJ. Two secreted retinal factors regulate different stages of development of the outer blood-retinal barrier. *Brain Res Dev Brain Res*. 2000;119(2):259–267.
23. Sun R, Peng S, Chen X, Zhang H, Rizzolo LJ. Diffusible retinal secretions regulate the expression of tight junctions and other diverse functions of the retinal pigment epithelium. *Mol Vis*. 2008;14:2237–2262.
24. Rizzolo LJ. Polarization of the Na^+K^+-ATPase in epithelia derived from the neuroepithelium. *Int Rev Cytol*. 1999;185:195–235.
25. Rizzolo LJ, Zhou S, Li Z-Q. The neural retina maintains integrins in the apical membrane of the RPE early in development. *Invest Ophthalmol Vis Sci*. 1994;35(5):2567–2576.
26. Kador KE, Goldberg JL. Scaffolds and stem cells: delivery of cell transplants for retinal degenerations. *Expert Rev Ophthalmol*. 2012;7(5):459–470.
27. Kundu J, Michaelson A, Talbot K, Baranov P, Young MJ, Carrier RL. Decellularized retinal matrix: natural platforms for human retinal progenitor cell culture. *Acta Biomater*. 2016;31:61–70.
28. Yao J, Ko CW, Baranov PY, et al. Enhanced differentiation and delivery of mouse retinal progenitor cells using a micropatterned biodegradable thin-film polycaprolactone scaffold. *Tissue Eng Part A*. 2015;21(7–8):1247–1260.
29. Goodson NB, Park KU, Silver JS, Chiodo VA, Hauswirth WW, Brzezinski JA. Prdm1 overexpression causes a photoreceptor fate-shift in nascent, but not mature, bipolar cells. *Dev Biol*. 2020;464(2):111–123.
30. Liu IS, JD Chen, Ploder L, et al. Developmental expression of a novel murine homeobox gene (Chx10): Evidence for roles in determination of the neuroretina and inner nuclear layer. *Neuron*. 1994;13(2):377–393.
31. Mu X, Klein WH. A gene regulatory hierarchy for retinal ganglion cell specification and differentiation. *Semin Cell Dev Biol*. 2004;15(1):115–123.
32. de Melo J, Zibetti C, Clark BS, et al. Lhx2 is an essential factor for retinal gliogenesis and notch signaling. *J Neurosci*. 2016;36(8):2391–2405.
33. Ekström P, Johansson K. Differentiation of ganglion cells and amacrine cells in the rat retina: correlation with expression of HuC/D and GAP-43 proteins. *Brain Res Dev Brain Res*. 2003;145(1):1–8.
34. Baylor DA, Burns ME. Control of rhodopsin activity in vision. *Eye (Lond)*. 1998;12(Pt 3b):521–525.
35. Furukawa T, Morrow EM, Cepko CL. Crx, a novel otx-like homeobox gene, shows photoreceptor-specific expression and regulates photoreceptor differentiation. *Cell*. 1997;91(4):531–541.
36. Singh D, Wang SB, Xia T, et al. A biodegradable scaffold enhances differentiation of embryonic stem cells into a thick sheet of retinal cells. *Biomaterials*. 2018;154:158–168.
37. Balasubramani M, Schreiber EM, Candiello J, Balasubramani GK, Kurtz J, Halfter W. Molecular interactions in the retinal basement membrane system: a proteomic approach. *Matrix Biol*. 2010;29(6):471–483.
38. Pinzón-Duarte G, Daly G, Li YN, Koch M, Brunken WJ. Defective formation of the inner limiting membrane in laminin beta2- and gamma3-null mice produces retinal dysplasia. *Invest Ophthalmol Vis Sci*. 2010;51(3):1773–1782.
39. Libby RT, Champliaud M-F, Claudepierre T, et al. Laminin expression in adult and developing retinae: evidence of two novel CNS laminins. *J Neurosci*. 2000;20(17):6517–6528.
40. Polisetti N, Sorokin L, Okumura N, et al. Laminin-511 and -521-based matrices for efficient ex vivo-expansion of human limbal epithelial progenitor cells. *Sci Rep*. 2017;7(1):5152.

Investigative Ophthalmology & Visual Science

41. Laperle A, Hsiao C, Lampe M, et al. α-5 Laminin synthesized by human pluripotent stem cells promotes self-renewal. *Stem Cell Rep*. 2015;5(2):195–206.
42. Byström B, Virtanen I, Rousselle P, Gullberg D, Pedrosa-Domellöf F. Distribution of laminins in the developing human eye. *Invest Ophthalmol Vis Sci*. 2006;47(3):777–785.
43. Dorgau B, Felemban M, Sharpe A, et al. Laminin γ3 plays an important role in retinal lamination, photoreceptor organisation and ganglion cell differentiation. *Cell Death Dis*. 2018;9(6):615–615.
44. Peng S, Gan G, Qiu C, et al. Engineering a blood-retinal barrier with human embryonic stem cell-derived retinal pigment epithelium: transcriptome and functional analysis. *Stem Cells Transl Med*. 2013;2(7):534–544.
45. Idelson M, Alper R, Obolensky A, et al. Directed differentiation of human embryonic stem cells into functional retinal pigment epithelium cells. *Cell Stem Cell*. 2009;5(4):396–408.
46. Livak KJ, Schmittgen TD. Analysis of relative gene expression data using real-time quantitative PCR and the 2(-Delta Delta C(T)) method. *Methods*. 2001;25(4):402–408.
47. Singh R, Phillips MJ, Kuai D, et al. Functional analysis of serially expanded human iPS cell-derived RPE cultures. *Invest Ophthalmol Vis Sci*. 2013;54(10):6767–6778.
48. Hazim RA, Karumbayaram S, Jiang M, et al. Differentiation of RPE cells from integration-free iPS cells and their cell biological characterization. *Stem Cell Res Ther*. 2017;8(1):217.
49. Saini JS, Corneo B, Miller JD, et al. Nicotinamide ameliorates disease phenotypes in a human iPSC model of age-related macular degeneration. *Cell Stem Cell*. 2017;20(5):635–647.e7.
50. Strunnikova NV, Maminishkis A, Barb JJ, et al. Transcriptome analysis and molecular signature of human retinal pigment epithelium. *Hum Mol Genet*. 2010;19(12):2468–2486.
51. Ostrer H, Pullarkat RK, Kazmi MA. Glycosylation and palmitoylation are not required for the formation of the X-linked cone opsin visual pigments. *Mol Vis*. 1998;4:28.
52. Kazmi MA, Sakmar TP, Ostrer H. Mutation of a conserved cysteine in the X-linked cone opsins causes color vision deficiencies by disrupting protein folding and stability. *Invest Ophthalmol Vis Sci*. 1997;38(6):1074–1081.
53. Wahlin KJ, Maruotti JA, Sripathi SR, et al. Photoreceptor outer segment-like structures in long-term 3D retinas from human pluripotent stem cells. *Sci Rep*. 2017;7(1):766.
54. Zhong X, Gutierrez C, Xue T, et al. Generation of three-dimensional retinal tissue with functional photoreceptors from human iPSCs. *Nat Commun*. 2014;5:4047.
55. Hallam D, Hilgen G, Dorgau B, et al. Human-induced pluripotent stem cells generate light responsive retinal organoids with variable and nutrient-dependent efficiency. *Stem Cells*. 2018;36(10):1535–1551.
56. Capowski EE, Samimi K, Mayerl SJ, et al. Reproducibility and staging of 3D human retinal organoids across multiple pluripotent stem cell lines. *Development*. 2019;146(1):dev171686.
57. Gordon PJ, Yun S, Clark AM, Monuki ES, Murtaugh LC, Levine EM. Lhx2 balances progenitor maintenance with neurogenic output and promotes competence state progression in the developing retina. *J Neurosci*. 2013;33(30):12197–12207.
58. Fields MA, Del Priore LV, Adelman RA, Rizzolo LJ. Interactions of the choroid, Bruch's membrane, retinal pigment epithelium, and neurosensory retina collaborate to form the outer blood-retinal-barrier. *Prog Retin Eye Res*. 2020;76:100803.
59. Rizzolo LJ, Peng S, Luo Y, Xiao W. Integration of tight junctions and claudins with the barrier functions of the retinal pigment epithelium. *Prog Retin Eye Res*. 2011;30(5):296–323.
60. Liao J-L, Yu J, Huang K, et al. Molecular signature of primary retinal pigment epithelium and stem-cell-derived RPE cells. *Hum Mol Genet*. 2010;19(21):4229–4238.
61. Ban Y, Rizzolo LJ. Differential regulation of tight junction permeability during development of the retinal pigment epithelium. *Am J Physiol*. 2000;279(3):C744–C750.
62. Gamm DM, Melvan JN, Shearer RL, et al. A novel serum-free method for culturing human prenatal retinal pigment epithelial cells. *Invest Ophthalmol Vis Sci*. 2008;49(2):788–799.
63. Hendrickson A. Development of retinal layers in prenatal human retina. *Am J Ophthalmol*. 2016;161:29–35.e21.
64. Hendrickson A, Drucker D. The development of parafoveal and mid-peripheral human retina. *Behav Brain Res*. 1992;49(1):21–31.

Investigative Ophthalmology & Visual Science